

## Stark-shift microscopy of single emitters

S. Karotke, A. Lieb, and B. Hecht<sup>a)</sup>

*Nano-Optics Group, National Center of Competence for Research in Nanoscale Science, Institute of Physics, University of Basel, Klingelbergstrasse 82, CH-4056 Basel, Switzerland*

(Received 9 January 2006; accepted 1 June 2006; published online 12 July 2006)

We study the interaction of a biased, metallized tip in close proximity to single fluorescent molecules at cryogenic temperature. By scanning over the sample, the tip's inhomogeneous electric field induces Stark shifts of the zero-phonon lines of nearby molecules. When illuminated with an off-resonant laser, molecules are tuned into resonance for specific tip positions located on circular patterns around the molecules' spatial positions. The origins of circles belonging to different molecules can be determined with high precision. We demonstrate a spatial resolution of neighboring individual molecules of  $\sim 50$  nm using a tip scanned in a distance of  $\sim 3$   $\mu\text{m}$  above the sample. © 2006 American Institute of Physics. [DOI: 10.1063/1.2219137]

The spatial resolution in optical imaging is limited by diffraction to about half the wavelength. Super-resolution imaging may be achieved by taking advantage of optical near fields bound to material structures, such as apertures<sup>1</sup> and sharp tips.<sup>2,3</sup> Alternatively, by taking advantage of *a priori* knowledge of the sample, e.g., its distinct spectral properties,<sup>4</sup> it is possible to achieve very high spatial resolution<sup>5</sup> and precise position measurements.<sup>6</sup>

Certain fluorescent molecules doped into crystalline matrices at cryogenic temperature exhibit very narrow zero-phonon absorption lines. The homogeneous broadening of the ensemble of molecules in a matrix allows to address individual molecules by means of a narrowband tunable laser.<sup>7</sup> The extreme sharpness of the zero-phonon lines allows the sensitive detection of minute spectral changes. The linear or quadratic Stark shift of a molecule's zero-phonon line in presence of an electric field can be used to externally tune the molecule's transition frequency.<sup>8,9</sup> Since the Stark shift depends on the electric field strength at the molecule's position, inhomogeneous electric fields, e.g., in the vicinity of sharp tips, lead to Stark shifts that depend on the relative spatial position of tip and molecule. As a consequence, the transition frequency of single molecules can be tuned over a wide range by nanometer precise positioning of a biased tip with respect to the molecule. If the laser frequency is kept fixed, a molecule may be pushed into resonance by appropriate positioning of the biased tip. We show that the characteristic fluorescence patterns, obtained as a function of tip position, to a first approximation are circles with a molecule at their origins. Multiple circles can be used to determine the position of nearby molecules. We achieve a precision of position determination of about 50 nm in a single scan, albeit unperturbed molecular resonance frequencies differ considerably and the gap width is around 3  $\mu\text{m}$ .

The setup consists of a sample-scanning confocal microscope combined with a scanning tip setup operating at cryogenic temperature. The setup is sketched in Fig. 1 and has been described in detail elsewhere.<sup>10,11</sup> In brief, the light of a single-mode tunable dye laser is directed into the cryostat and is then focussed onto the sample by a microscope objective (Microthek, numerical aperture (NA)=0.85). Redshifted

fluorescence is collected with the same objective and detected by a single-photon counting avalanche photodiode. Excitation light is blocked by a notch filter. On top of the confocal microscope, the scanning tip setup is mounted. The tip is an etched glass fiber<sup>12</sup> metallized by 40 nm of silver. The tip apex has a diameter of about 60 nm. To align the tip within the focal volume of the confocal microscope, light is coupled into the far end of the glass fiber as to illuminate the tip. The tip is then approached to the sample and positioned laterally such that its image approximately superimposes with the reflected confocal spot in the detector plane. The sample consists of *p*-terphenyl microcrystals doped with terylene, produced in a similar way as described in Ref. 13. 2/3 of a slightly oversaturated terylene-toluene solution and 1/3 of a *p*-terphenyl-toluene solution are mixed in an ultrasonic bath. A droplet of 25  $\mu\text{l}$  of the mixed solution is then spin coated onto a thin glass plate. This method yields microcrystals ( $\sim 1$ –4  $\mu\text{m}^2$ ) with a thickness between 50 and 150 nm, measured by atomic force microscopy (AFM).

With the confocal setup we are able to scan the sample in a range of about  $10 \times 10$   $\mu\text{m}^2$  at cryogenic temperature. A suitable microcrystal, preferentially holding multiple mol-

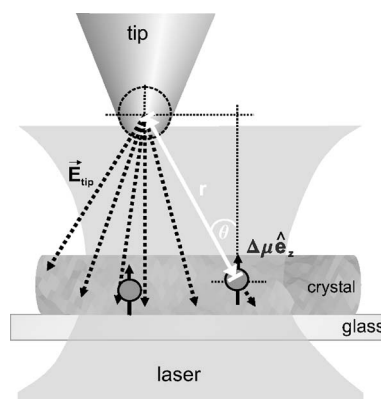


FIG. 1. Sketch of the experimental setup, showing the geometry of the tip (described as a sphere) and two molecules (described as two single dipoles) in the laser focus. Illustration of the influence of the two parameters to the Stark shift: the distance  $r$  between the tip and the emitter and the angle  $\theta$  between  $\Delta\mu\hat{\epsilon}_z$  and  $\mathbf{E}_{\text{tip}}$ . For details, see text.

<sup>a)</sup>Electronic mail: bert.hecht@nano-optics.ch

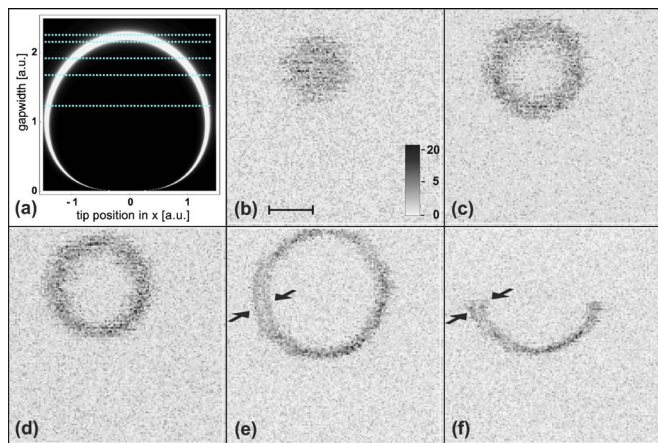


FIG. 2. (a) Vertical section along the  $z$  axis at  $y=0$  of the calculated fluorescence of a single emitter depending on the tip position. The voltage and the detuning are kept constant. The five lines represent sections at different heights, where the experimental measurements have been taken. [(b)–(f)] Fluorescence depending on the tip position at different gap widths. The scale bar is  $1 \mu\text{m}$ , the grayscale is in counts. The arrows in (e) and (f) indicate a splitting of the ring.

ecules with differing resonance frequencies, is then moved into the laser focus for further investigation. The laser is set to a frequency within the photostable  $X_2$  site at  $\approx 17\,286 \text{ cm}^{-1}$  that is not in resonance with any of the single-molecules' zero-phonon lines. The tip is positioned in the vicinity of the focal spot ( $\varnothing \sim 400 \text{ nm}$ ) such that a full-range tip scan ( $5 \times 5 \mu\text{m}^2$ ) includes the position of the focus. When the biased tip now scans over the area of interest, it pushes molecules in and out of resonance with the laser frequency.

Figures 2(b)–2(f) present a series of Stark-shift images with only one molecule in the laser focus, showing the recorded fluorescence as a function of tip position. Each image is taken at a different gap widths  $z$  until in Fig. 2(f), the molecule photobleaches. Reducing the gap width results in an increase of the diameter and a decrease of the width of the circular fluorescence pattern. A simple theoretical model accounts for this behavior. We consider a single emitter, located at the center of the  $(x, y)$  scan of the tip. The emitter exhibits matrix-induced permanent dipole moment difference  $\Delta\mu\hat{e}_z$ , oriented along the  $z$  direction (Fig. 1). The tip is modeled as a charged sphere with radius of about  $60 \text{ nm}$ . The dipole-laser interaction, leading to fluorescence, is calculated using the density matrix approach.<sup>14</sup> Accounting for a linear Stark shift,  $\hbar\Delta\nu = -\Delta\mu\hat{e}_z\mathbf{E}(x, y, z)$ , depending on the tip position via the electric field  $\mathbf{E}(x, y, z)$  leads to

$$\Delta\nu = F \frac{\Delta\mu z}{\hbar[(x-x_0)^2 + (y-y_0)^2 + z^2]^{3/2}}. \quad (1)$$

Here  $(x, y, z)$  describes the tip position in three dimensions,  $(x_0, y_0)$  is the position of the emitter, and  $F$  is a parameter taking into account the applied voltage and the tip geometry. We obtain an expression for the fluorescence depending on tip position by introducing the tip-position-dependent Stark shift (1) into the formula for the emission rate  $f$ ,

$$f(x, y, z) = b + \frac{\omega_R^2 \Gamma}{2\omega_R^2 + \Gamma^2 + 4(\Delta\tilde{\nu} - \Delta\nu)^2}. \quad (2)$$

Here,  $b$  is a background,  $\omega_R$  the Rabi frequency,  $\Gamma$  the line width of the molecule, and  $\Delta\tilde{\nu}$  the laser detuning. The model predicts fluorescence patterns as a function of the tip position and gap width. A cross section in the  $(x-z)$  plane of Eq. (2) is plotted in Fig. 2(a). As the tip approaches, the ring width decreases and the diameter increases concomitantly, in accordance with the experimental findings. It is obvious that the coupling of the electric field to the dipole depends on the distance  $r$  and on the angle  $\theta$  between  $\Delta\mu\hat{e}_z$  and  $\mathbf{E}$  (Fig. 1). By approaching the biased tip, the field strength at the position of the molecule increases, which results in an enlargement of the Stark-shift ring. At a certain critical gapwidth the angle  $\theta$  between  $\mathbf{E}$  and  $\Delta\mu\hat{e}_z$  becomes unfavorable. Only the stronger field in closer proximity to the tip apex induces a Stark shift sufficiently strong to push the molecule into resonance. This results in a decrease of the Stark-shift ring diameter. The measured and simulated decrease in the width of the Stark-shift ring can be explained by the increase of the field gradient during the tip approach.

Significant lateral components of the permanent dipole moment difference would lead to elliptical patterns instead of rings, which are not observed experimentally. Asymmetries of the Stark-shift pattern are expected if the molecule shows a quadratic or higher order Stark shift behavior. However, such asymmetries become important only at gap widths of  $d < 3 \mu\text{m}$ .

On the left hand side in Figs. 2(e) and 2(f), a splitting of the Stark-shift ring is seen, as indicated by the arrows. This splitting of the Stark-shift ring is attributed to the presence of a two-level system (TLS) in the matrix close to the molecule, whose flipping rate can be influenced by the electric field of the probe.<sup>15,16</sup> The splitting can be reproduced numerically by assuming a single molecule coupled to a nearby TLS.<sup>17,18</sup>

If more than one molecule is present in the focal volume, the positions of molecules and their respective distances can be determined with high accuracy taking advantage of the spectral information. Figure 3(a) shows a regular fixed-frequency confocal image of a sample containing several fluorescent spots. A typical frequency scan obtained in this sample area is shown in Fig. 3(b). Three spectrally separated molecules are detected within the excitation volume. Their line widths are between  $30$  and  $38 \text{ MHz}$  and their spectral separation is  $\Delta\nu_1 = 420 \text{ MHz}$  and  $\Delta\nu_2 = 170 \text{ MHz}$ , respectively. By scanning the biased tip ( $V = -180 \text{ V}$ ) with an initially off-resonant laser frequency, the presence of three molecules is apparent in one spatial tip scan [Figs. 3(c)–3(f)]. One molecule shows spectral jumps, evident from the interruptions and abrupt changes in diameter of the outer ring. This instability has an impact on the other two molecules, as can be seen best in Fig. 3(d), indicated by the arrows. The ring width broadens for both inner Stark-shift rings and the radii are reduced. This could be explained by a strong dipole-dipole coupling between all three molecules.<sup>9</sup>

During the experiment, the tip was approached from  $4.11$  to  $3.12 \mu\text{m}$ . The gap width  $z$  is obtained from Stark-shift measurements, where only the voltage applied the tip is varied and the distance  $z$  as well as the detuning  $\Delta\tilde{\nu}$  are kept constant. The two inner rings, whose origins coincide with the molecules' positions, seem to be centered. However,

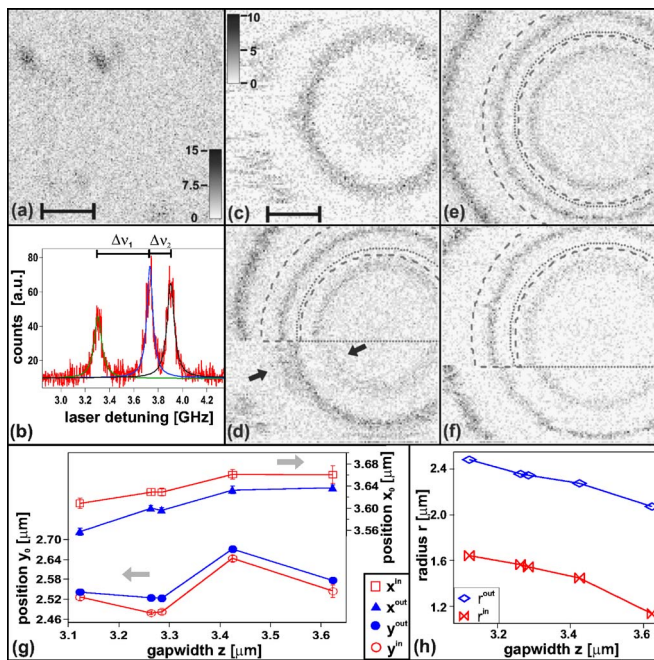


FIG. 3. (a) Confocal image (1.4 K,  $17\,285.8\text{ cm}^{-1}$ ). Scale bar is  $2\ \mu\text{m}$ , grayscale is in counts. (b) Spectrum with three spectrally distinguishable molecules. Solid lines are fits of the resonances and  $\Delta\nu_1$  and  $\Delta\nu_2$  are the relative spectral separation, see text. [(c)–(f)] Stark-shift images of the three molecules in the focus at different distances  $z$ ,  $z=4.11\pm 0.23\ \mu\text{m}$  (c),  $z=3.42\pm 0.23\ \mu\text{m}$  (d),  $z=3.26\pm 0.23\ \mu\text{m}$  (e), and  $z=3.12\pm 0.23\ \mu\text{m}$  (f). Scale bar is  $1\ \mu\text{m}$ , grayscale is in counts. Fit masks are outlined by a dashed line for the outer ring and a dotted line for the inner ring, respectively. (g)  $(x_0, y_0)$  positions for two of the three molecules depending on the gap width. (h) Increase of the radius depending on the gap width.

careful analysis reveals that the two molecules are clearly separated by an average distance of  $\bar{r} = \sqrt{\Delta x_0^2 + \Delta y_0^2} = 46 \pm 11\ \text{nm}$ . The origins of the rings are obtained by non-linear fitting of the rings according to Eq. (2). The fits have been restricted to areas, where the outer molecule shows a stable spectral behavior, as indicated by the fit masks in Fig. 3. The values for  $x_0$  and  $y_0$  in Fig. 3(g) vary during the approach. This is assigned to lateral jumps of the slip-stick

drive which is used for the tip approach. Evidence for this explanation is the fact that the values for both molecules shift parallel. Figure 3(h) shows the increase of the Stark-shift ring radii as expected from the numerical simulation.

The authors gratefully acknowledge H.-J. Güntherodt for his continuous support as well as helpful discussions with C. Schroll for the theoretical calculations, AFM measurements by V. Thommen, and support by J. Y. P. Butter. Financial support is acknowledged by the Swiss National Science Foundation via the National Center of Competence in Research (NCCR) in Nanoscale Science and a research professorship for one of the authors (B.H.).

<sup>1</sup>B. Hecht, B. Sick, U. P. Wild, V. Deckert, R. Zenobi, O. J. F. Martin, and D. W. Pohl, *J. Chem. Phys.* **112**, 7761 (2000).

<sup>2</sup>A. Hartschuh, E. J. Sánchez, X. S. Xie, and L. Novotny, *Phys. Rev. Lett.* **90**, 095503 (2003).

<sup>3</sup>F. Keilmann and R. Hillenbrand, *Philos. Trans. R. Soc. London, Ser. A* **362**, 787 (2004).

<sup>4</sup>E. Betzig, *Opt. Lett.* **20**, 237 (1995).

<sup>5</sup>T. A. Klar, S. Jakobs, M. Dyba, A. Egner, and S. W. Hell, *Proc. Natl. Acad. Sci. U.S.A.* **97**, 8206 (2000).

<sup>6</sup>A. Yildiz, J. N. Forkey, S. A. McKinney, T. Ha, Y. E. Goldman, and P. R. Selvin, *Science* **300**, 2061 (2003).

<sup>7</sup>W. E. Moerner and M. Orrit, *Science* **283**, 1670 (1999).

<sup>8</sup>U. P. Wild, F. Güttler, M. Pirota, and A. Renn, *Chem. Phys. Lett.* **193**, 452 (1992).

<sup>9</sup>C. Hettich, C. Schmitt, J. Zitzmann, S. Kühn, I. Gerhardt, and V. Sandoghdar, *Science* **298**, 385 (2002).

<sup>10</sup>J.-M. Segura, A. Renn, and B. Hecht, *Rev. Sci. Instrum.* **71**, 1706 (2000).

<sup>11</sup>A. Kramer, J.-M. Segura, A. Hunkeler, A. Renn, and B. Hecht, *Rev. Sci. Instrum.* **73**, 2937 (2002).

<sup>12</sup>R. Stöckle, C. Fokas, V. Deckert, R. Zenobi, B. Sick, B. Hecht, and U. P. Wild, *Appl. Phys. Lett.* **75**, 160 (1999).

<sup>13</sup>R. J. Pfab, J. Zimmermann, C. Hettich, I. Gerhardt, A. Renn, and V. Sandoghdar, *Chem. Phys. Lett.* **387**, 490 (2004).

<sup>14</sup>L. Mandel and E. Wolf, *Optical Coherence and Quantum Optics* (Cambridge University Press, Cambridge, 1995).

<sup>15</sup>H. Maier, R. Wunderlich, D. Haarer, B. M. Kharlamov, and S. G. Kulikov, *Phys. Rev. Lett.* **74**, 5252 (1995).

<sup>16</sup>J.-M. Segura, G. Zumofen, A. Renn, B. Hecht, and U. P. Wild, *Chem. Phys. Lett.* **340**, 77 (2001).

<sup>17</sup>E. Geva and J. L. Skinner, *J. Chem. Phys.* **109**, 4920 (1998).

<sup>18</sup>M. Bauer and L. Kador, *J. Chem. Phys.* **118**, 9069 (2003).